#### G Model APSUSC-36173; No. of Pages 8

## **ARTICLE IN PRESS**

Applied Surface Science xxx (2017) xxx-xxx

ELSEWIED

Contents lists available at ScienceDirect

### **Applied Surface Science**

journal homepage: www.elsevier.com/locate/apsusc



#### Full Length Article

# Structure and tribological properties of argon arc cladding Ni-based nanocrystalline coatings

Jun-sheng Meng<sup>a,b,\*</sup>, Guo Jin<sup>a</sup>, Xiao-ping Shi<sup>b</sup>

- <sup>a</sup> College of Materials Science and Chemical Engineering, Harbin Engineering University, Harbin, 150001, China
- b School of Materials Science & Engineering, Heilongjiang University of Science and Technology, Harbin, 150022, China

#### ARTICLE INFO

#### Article history: Received 22 February 2017 Received in revised form 20 April 2017 Accepted 27 May 2017 Available online xxx

Keywords: Argon arc cladding Nanocrystalline Microstructure Tribological properties

#### ABSTRACT

TiN-TiB<sub>2</sub> nanocrystalline coatings have been in-situ synthesized on the 35CrMnSi steel surface by argon arc cladding process under different welding technological parameters. The calculating method was established for the analysis and calculation of the dilution ratio. The microstructures of the nanocrystalline coatings were characterized by means of X-ray diffraction meter(XRD), scanning electron microscopy (SEM) and transmission electron microscopy (TEM).Results indicated that the phase of coatings were TiN TiB<sub>2</sub> TiB  $Cr_{23}C_6$  and  $\gamma$ -Ni. The welding technological parameters of nanocrystalline coatings have certain effects on the dilution ratio of the clad layer. The tribological behavior of both the substrate and the coatings was investigated in detail. An average microhardness of 1420HV<sub>0.5</sub> was obtained with a cladding current of 120A. While the nanocrystalline coatings shows better wear resistance properties than 35CrMnSi steel.

© 2017 Elsevier B.V. All rights reserved.

#### 1. Introduction

Nanocrystalline composites have superior mechanical properties and high wear and corrosion resistance, thereby enhancing the high strength, hardness, and plasticity of nanocrystalline materials. The in-situ synthesis of metal matrix composites is highly studied due to its high bonding strength with the matrix, pollution-free interface, and uniform particle distribution. Both TiN and TiB<sub>2</sub> in the particle reinforced phase are used in wear-resistant structural parts designed for ultra-high temperature conditions because of their high hardness, high melting point, good chemical stability at high temperatures, and good corrosion resistance and abrasion resistance at high temperatures [4].

TiN-TiB<sub>2</sub> nanocrystalline coatings have been prepared by laser cladding, plasma deposition, and self-propagating high-temperature synthesis techniques [5–7]. However, these methods have complicated operations and require a high equipment cost, thus increasing the manufacturing cost. The research of argon arc welding technology has significantly increasing in recent years [8–14]. Soner et al. prepared a WC enhanced nickel matrix-based composite coating on the surface of stainless steel by the argon arc welding technique [15]. Mridha S combined titanium powder and aluminum powder to create a welding material for the preparation

[16]. Those researches on the argon arc welding technique were focused on the structure and properties of particles at the micrometer level. It is significant to study the variation of microstructures of the coatings and discuss the formation mechanisms under different processing conditions. The present study employed the in-situ argon arc welding and rapid cooling methods to deposit titanium powder, boron nitride powder, and Ni60A powder on the surface of 35CrMnSi to synthesize nanocrystalline Ni-based composite coatings. The influence of the argon arc welding parameters on the dilution rate, phase composition, microstructure, and properties of the coating was analyzed.

of a Ti3Al enhanced titanium matrix-based composite coating on the surface of pure titanium using the argon arc welding technique

#### 2. Experimental

#### 2.1. Argon arc cladding processing

The 35CrMnSi steel (composition: 0.31 wt.%C, 1.13 wt.%Mn, 1.15 wt.%Si, 1.25 wt.%Cr and Fe balance) was used as the substrate material with a dimension of  $80 \, \text{mm} \times 25 \, \text{mm} \times 10 \, \text{mm}$ , which need be polished with 100-grit SiC abrasive paper and degreased in acetone and alcohol prior to coating. The powers used for depositing process were a mixture of BN (99.5% purity, 1.0  $\mu$ m), Titanium powders (99.5% purity,  $\sim$ 20  $\mu$ m) and Ni60(composition: 0.62 wt.%C, 15.45 wt.%Cr, 4.42 wt.%Si, 3.20 wt.%Fe, 3.50 wt.%B and Ni balance,  $\sim$ 50  $\mu$ m). The powders were proportioned in molar ratios of BN/Ti = 0.67, respectively. The mass ratio of Ni60 and (Ti+BN) was

http://dx.doi.org/10.1016/j.apsusc.2017.05.238 0169-4332/© 2017 Elsevier B.V. All rights reserved.

<sup>\*</sup> Corresponding author at: School of Materials Science & Engineering, Heilongjiang Institute of Science and Technology, Harbin, 150027, China. E-mail address: mengjs2008@163.com (J.-s. Meng).

## ARTICLE IN PRESS

J.-s. Meng et al. / Applied Surface Science xxx (2017) xxx-xxx

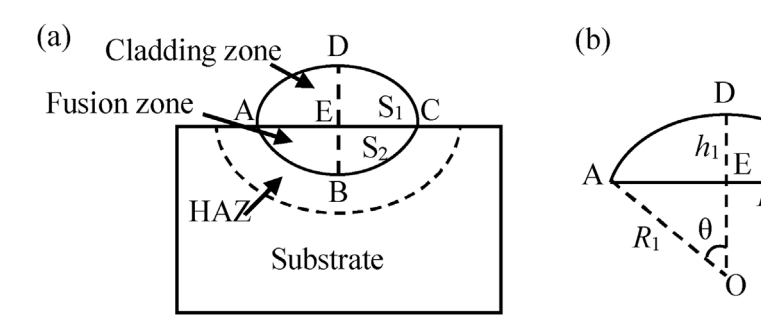


Fig. 1. Schematic diagram for calculating the dilution rate of the surface coating (a) Transverse profile of the coated surface and (b) method for computing the value of area S<sub>1</sub>

**Table 1**The parameters of argon arc cladding.

Welding current (A)	Welding speed (mm/min)	Velocity of powder feeding (g/min)	Argon flow rate (L/min)
100-160	60-240	10	12

80:20. These powders were dry-mixed for 10 h in a planetary ball mill (type, DECO-PBM-V-2L-A). Then coatings were carried out by MW3000 Digital Tungsten Inert Gas welding machine. To obtain a good interface fusion, a smooth coating surface and a minimum dilution, the parameters of argon arc cladding are shown in Table 1. The Argon was used as gas medium to feed the powder which could protect alloy powers from oxidation during the process of argon arc cladding. The samples were cooled by HK2009-MT800 water circulator during cladding process.

#### 2.2. Microanalysis

XD-2 X-ray diffractrometric was used to analyze the phase structure of the coatings with Cu K $\alpha$  irradiation ( $\lambda$ =0.1540 nm) while the scanning speed was 4° per minute and the step size was 0.02°. The microstructure of the coatings was visualized with a MX-2600 SEM. Samples for transmission electron microscopy (TEM) were cut from the cladding coating. Subsequently, they were polished to a 100  $\mu$ m thickness with SiC paper. The samples were punched to 3 mm disc samples and dimple ground to 20  $\mu$ m thickness. This was followed by ion milling, which used Ar<sup>+</sup> bombardment at 5 keV using a Gatan Precision Polishing System. TEM observations were performed using a Tecnai G2 F20 TEM operating at 200 KV.

#### 2.3. Performance testing

A Vickers hardness tester (MHV-2000) was used to measure the micro-hardness of nanocrystalline coatings The load was 4.90 N and loading time was 10s. A friction wear testing machine (MMS-2A) was used to measure the wear properties of the coatings at the room temperature and normal atmosphere condition. The test coating specimens were machined with size of  $10\,\mathrm{mm}\times5\,\mathrm{mm}\times5\,\mathrm{mm}$ . A GCr15 steel with the hardness of HRC60 was used as the friction counterpart. The wear conditions were a normal load of 200 N, a sliding speed of  $200\,\mathrm{r/min}$ , and the time of abrasion of  $120\,\mathrm{min}$ .

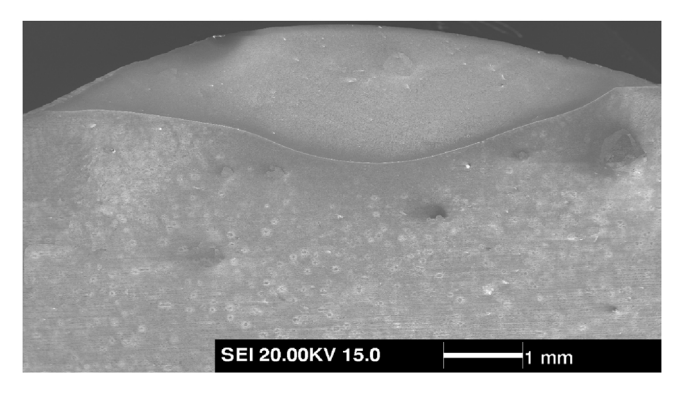


Fig. 2. The cross-sectional profile of the cladding coating.

#### 3. Results and discussion

#### 3.1. Calculation of dilution ratio

Welding involves the melting of a base metal. A change in the composition of the cladding coating due to the addition of a melted base material is generally described by the dilution ratio (d), which is calculated by Eq. (1).

$$d = \frac{S_2}{S_1 + S_2} \tag{1}$$

Where d stands for the value of coating dilution,  $S_1$  refers to the area of the pre-coating and  $S_2$  represents the area of fused metal matrix respectively.

Fig. 1 shows the illustration of the transverse profile for the coated surface. The equation for the dilution ratio was derived based on reference [17]. The ADC and ABC curves can be treated as an arc if the energy input is assumed to follow a normal distribution. In this case, the area of  $S_1$  was calculated by subtracting the triangle OAC from the area OADC. The cross-sectional profile was obtained by SEM. Fig. 2 shows the representative microstructure of coating's cross-section produced by argon arc cladding with 120 A current and 120 mm/min, which exhibited the absence of a bubble, crack, or impurity at the interface between the welding layer and matrix.

The dilution ratio of the cross-section in the welding layer was calculated based on the corresponding data and Eq. (2), of which the impact of the welding current and welding speed on the dilution ratio were analyzed, as illustrated in Fig. 3.

$$I = \frac{1}{1 + (h_1/h_2)^2 \left\{ \frac{((K_1^2 + 4)2 \arctan[4K_1/(K_1^2 - 4)] - 4K_1(K_1^2 - 4)]((K_2^2 + 4)^2 \arctan[4K_2/(K_2^2 - 4)] - 4K_2(K_2^2 - 4)}{1 + (h_1/h_2)^2 \left\{ \frac{((K_1^2 + 4)2 \arctan[4K_1/(K_1^2 - 4)] - 4K_1(K_1^2 - 4)]((K_2^2 + 4)^2 \arctan[4K_2/(K_2^2 - 4)] - 4K_2(K_2^2 - 4)}{1 + (h_1/h_2)^2 \left\{ \frac{((K_1^2 + 4)2 \arctan[4K_1/(K_1^2 - 4)] - 4K_1(K_1^2 - 4)]((K_2^2 + 4)^2 \arctan[4K_2/(K_2^2 - 4)] - 4K_2(K_2^2 - 4)}{1 + (h_1/h_2)^2 \left\{ \frac{((K_1^2 + 4)2 \arctan[4K_1/(K_1^2 - 4)] - 4K_1(K_1^2 - 4)]((K_2^2 + 4)^2 \arctan[4K_2/(K_2^2 - 4)] - 4K_2(K_2^2 - 4)}{1 + (h_1/h_2)^2 \left\{ \frac{((K_1^2 + 4)2 \arctan[4K_1/(K_1^2 - 4)] - 4K_1(K_1^2 - 4)]((K_2^2 + 4)^2 \arctan[4K_2/(K_2^2 - 4)] - 4K_2(K_2^2 - 4)}{1 + (h_1/h_2)^2 \left\{ \frac{((K_1^2 + 4)2 \arctan[4K_1/(K_1^2 - 4)] - 4K_1(K_1^2 - 4)]}{1 + (h_1/h_2)^2 \left\{ \frac{(K_1^2 + 4)2 \arctan[4K_1/(K_1^2 - 4)] - 4K_1(K_1^2 - 4)]}{1 + (h_1/h_2)^2 \left\{ \frac{(K_1^2 + 4)2 \arctan[4K_1/(K_1^2 - 4)] - 4K_1(K_1^2 - 4)]}{1 + (h_1/h_2)^2 \left\{ \frac{(K_1^2 + 4)2 \arctan[4K_1/(K_1^2 - 4)] - 4K_1(K_1^2 - 4)]}{1 + (h_1/h_2)^2 \left\{ \frac{(K_1^2 + 4)2 \arctan[4K_1/(K_1^2 - 4)] - 4K_1(K_1^2 - 4)]}{1 + (h_1/h_1)^2 \left\{ \frac{(K_1^2 + 4)2 \arctan[4K_1/(K_1^2 - 4)] - 4K_1(K_1^2 - 4)]}{1 + (h_1/h_1)^2 \left\{ \frac{(K_1^2 + 4)2 \arctan[4K_1/(K_1^2 - 4)] - 4K_1(K_1^2 - 4)]}{1 + (h_1/h_1)^2 \left\{ \frac{(K_1^2 + 4)2 \arctan[4K_1/(K_1^2 - 4)]}{1 + (h_1/h_1)^2 \left\{ \frac{(K_1^2 + 4)2 \arctan[4K_1/(K_1^2 - 4)] - 4K_1(K_1^2 - 4)]}{1 + (h_1/h_1)^2 \left\{ \frac{(K_1^2 + 4)2 \arctan[4K_1/(K_1^2 - 4)]}{1 + (h_1/h_1)^2 \left\{ \frac{(K_1^2 + 4)2 \arctan[4K_1/(K_1^2 - 4)]}{1 + (h_1/h_1)^2 \left\{ \frac{(K_1^2 + 4)2 \arctan[4K_1/(K_1^2 - 4)]}{1 + (h_1/h_1)^2 \left\{ \frac{(K_1^2 + 4)2 \arctan[4K_1/(K_1^2 - 4)]}{1 + (h_1/h_1)^2 \left\{ \frac{(K_1^2 + 4)2 \arctan[4K_1/(K_1^2 - 4)]}{1 + (h_1/h_1)^2 \left\{ \frac{(K_1^2 + 4)2 \arctan[4K_1/(K_1^2 - 4)]}{1 + (h_1/h_1)^2 \left\{ \frac{(K_1^2 + 4)2 \arctan[4K_1/(K_1^2 - 4)]}{1 + (h_1/h_1)^2 \left\{ \frac{(K_1^2 + 4)2 \arctan[4K_1/(K_1^2 - 4)]}{1 + (h_1/h_1)^2 \left\{ \frac{(K_1^2 + 4)2 \arctan[4K_1/(K_1^2 - 4)]}{1 + (h_1/h_1)^2 \left\{ \frac{(K_1^2 + 4)2 \arctan[4K_1/(K_1^2 - 4)]}{1 + (h_1/h_1)^2 \left\{ \frac{(K_1^2 + 4)2 \arctan[4K_1/(K_1^2 - 4)]}{1 + (h_1/h_1)^2 \left\{ \frac{(K_1^2 + 4)2 \arctan[4K_1/(K_1^2 - 4)]}{1 + (h_1/h_1)^2 \left\{ \frac{(K_1^2 + 4)2 \arctan[4K_1/(K_1^2 - 4)]}{1 + (h_1/h_1)^2 \left\{ \frac{(K_1/h_1)^2 \left\{ \frac$$

In Eq. (2),  $K_1$  equals to the radio of w and  $h_1$  and  $K_2$  stands for the radio computed of w and  $h_2$ ,  $h_1$  represents the maximum height

Please cite this article in press as: J.-s. Meng, et al., Structure and tribological properties of argon arc cladding Ni-based nanocrystalline coatings, Appl. Surf. Sci. (2017), http://dx.doi.org/10.1016/j.apsusc.2017.05.238

#### Download English Version:

## https://daneshyari.com/en/article/7836590

Download Persian Version:

https://daneshyari.com/article/7836590

Daneshyari.com